Critical uncoupling between biogeochemical stocks and rates in Ross Sea springtime production-export dynamics

Meredith G. Meyer[1,3], Esther Portela[1,2], Walker O. Smith Jr.[3,4], Karen J. Heywood[1]

[1]Centre for Ocean and Atmospheric Sciences, School of Environmental Sciences, University of East Anglia, Norwich, UK
[2]Laboratoire d'Oceanographie Physique et Spatiale, University of Brest, CNRS, IRD, Ifremer, Plouzané, France
[3]Virginia Institute of Marine Science, William & Mary, Gloucester Pt., VA, USA
[4]School of Oceanography, Shanghai Jiao Tong University, Shanghai, China

Correspondence to: Meredith Meyer (m.meyer@uea.ac.uk)

Abstract. Three biogeochemical glider surveys in the Ross Sea between 2010 and 2023 were combined and analysed to assess production-export stock and rate dynamics. As the most productive of any Antarctic continental shelf, the Ross Sea is a site of substantial physical and biogeochemical interest. While this region and its annual bloom have been characterised for decades, logistical constraints, such as ship time and sea ice cover, have prevented a comprehensive understanding of this region over long (>1-2 months) time scales and in high spatiotemporal resolution. Here we use high-resolution data sets from autonomous gliders in mass balance equations to calculate short-term (days to weeks) net community production via oxygen concentration, change in particulate organic carbon (POC) concentration over time, and POC export potential during the period of peak primary production in the region (November – February). Our results show an overall decoupling of net community production (NCP), driven by biologic changes in oxygen, from overall biomass concentration as well as changes in POC over time. NCP and carbon change vary between seasons and appear related to changes in ice concentration and stratification. Substantial spatiotemporal variability exists in all datasets, but high-resolution sampling reveals short term variations that are likely masked in other studies. Our study reinforces the need for high-resolution sampling and supports previous classifications of the Ross Sea as a high productivity (average NCP range -0.7 – 0.2 g C m^{-2} d^{-1}), low export (average changes in POC over time range -0.1 – 0.1 g C m^{-2} d^{-1}) system during the productive austral spring and sheds additional light on the mechanisms controlling these processes.

1 Introduction

The balance between organic carbon production and organic carbon export from the surface ocean has been intensely investigated in recent years because of the key role it plays in regulating global climate (Siegel et al., 2016; Henson et al., 2024). While long-term monitoring programmes have allowed certain oceanic regions to be well characterised (Karl and Church, 2014; Steinberg et al., 2001; Hartman et al., 2021), uncertainties surrounding these processes in certain regions, such as the Southern Ocean, have limited our global understanding of this balance. However, the proliferation of autonomous assets, such as autonomous underwater vehicles (AUVs), profiling floats, and gliders, equipped with biogeochemical sensors, have allowed more and new measurements of carbon production and export processes at very high spatial and temporal resolutions, in places where sampling is challenging (Kaufman et al., 2014; Alkire et al., 2014). Despite these substantial advances in recent years, some regions still lack a long history of high-resolution observations, making it difficult to differentiate between general trends or anomalous events in a system.

One of these regions is the Ross Sea, which is a key region for organic and inorganic carbon cycling but continues to lack a complete, long-term understanding of biogeochemical dynamics because of logistical constraints. Shipboard and modelled estimates of primary production (Smith et al., 2000; Smith et al., 2013; Schine et al., 2015), carbon concentrations (Sweeney et al., 2000), and carbon export (Nelson et al., 1996; Collier et al., 2000) have been conducted in the Ross Sea since the 1970s but have been limited to discrete sampling in select locations. Moreover, substantial cloudiness in the region limits ocean colour satellite retrievals in the Ross Sea. Satellite bio-optical algorithms are derived primarily from low and mid-latitude biogeochemical properties (Hu et al., 2019), making satellite biogeochemical measurements from the Ross Sea both difficult and frequently inaccurate because of the substantial differences between these properties in high versus low latitude regions (Chen et al., 2021).

Despite these limitations, the importance of the Ross Sea in Southern Ocean carbon cycling is clear. The Southern Ocean as a whole plays a disproportionately important role in global carbon dynamics, accounting for 40% of carbon uptake (DeVries, 2014), and the Ross Sea is responsible for 28% of that, despite only accounting for approximately 10% of the global ocean surface (Arrigo et al., 2008). An important metric for evaluating the relationship between primary production and carbon export is the total amount of carbon that is converted to biomass after losses associated with autotrophic and heterotrophic

respiration have been accounted for; this is termed net community production (NCP). Under steady-state conditions (i.e., carbon accumulation and loss terms are balanced over long timescales), NCP can be related to carbon export and is thus an important metric in evaluating production-export dynamics in oceanic systems (Cassar et al., 2015).

The Ross Sea is characterised by pronounced seasonal cycles dominated by a productive spring to summer season alternating with a comparatively unproductive autumn to winter season driven by heterotrophic processes. The productive period is dominated by a well-described, large and sustained phytoplankton bloom dominated by two key groups: colonial and solitary forms of the haptophytes *Phaeocystis antarctica* and diatoms (Smith et al., 2014). This bloom has been shown to reach substantial concentrations of biomass with chlorophyll concentrations reaching anywhere from 6 μg L^{-1} to >40 μg L^{-1} (Smith et al., 2000; Smith et al., 2011; Portela et al., 2025). Additionally, the region supports a substantial number of higher trophic levels, including Adelie and Emperor penguins, Orcas, Weddell, Crabeater, and Leopard seals, and pelagic birds (Smith et al., 2014).

The Ross Sea consistently exhibits high rates of primary production (Arrigo et al., 2008; Smith et al., 2014), but the ultimate fate of that biogenic carbon remains uncertain (Lo Monaco et al., 2005; Gruber et al., 2019). Along with the North Atlantic (Frigstad et al., 2015; Hartman et al., 2010) and upwelling regions (Demarcq, 2009), widespread phytoplankton blooms make the Southern Ocean continental shelf, during the bloom period, one of the most productive regions on the planet (Smith and Kaufman, 2018; Buesseler et al., 2020). Despite this, some studies have found reduced carbon transfer efficiencies relative to other regions on seasonal and annual timescales (e.g., flux transfer efficiencies ranging from 0.2 to 0.8; Buesseler et al., 2020). These findings are supported by modelling studies, thus leading to the classification of the Ross Sea as a high production, low export system (Henson et al., 2019).

We assess high-resolution carbon production and export dynamics in the Ross Sea from three independent glider deployments during the austral spring/summer in 2010 – 2011, 2012 – 2013, and 2022 – 2023 and calculate biogeochemical rates, including NCP, changes in particulate organic carbon (POC) over time ($\frac{\partial POC}{\partial t}$), and carbon export potential ($Export^{*}_{POC}$). We also evaluate POC : chlorophyll ratios (C:Chl) to assess how production-export dynamics have changed through time and how differences between deployments relate to taxonomic controls on production and export. The measurements evaluated come from glider-based dissolved oxygen, optical backscatter, and fluorescence data with the latter

Deleted: large

Deleted: particulate organic carbon

two converted to POC and chlorophyll concentrations, respectively. This study is the first to use consistent methodology to compare high-resolution estimates of carbon production and export processes from different years on the Ross Sea continental shelf, providing further understanding of the role the Ross Sea plays in Southern Ocean carbon dynamics.

2. Methods

2.1 Glider Deployments

Three deployments of autonomous Seagliders (Eriksen et al., 2001) equipped with biogeochemical sensors were completed in summer 2010 – 2011, 2012 – 2013, and 2022 – 2023 in the southwest Ross Sea (Fig. 1; Fig. 2). Observational periods coincided with the onset and the majority of the annual spring phytoplankton bloom with gliders surveying from 22 November to 20 January (2010-2011; Kaufman et al., 2014; Queste et al., 2015), 31 November to 6 February (2012-2013; Jones and Smith, 2017; Meyer et al., 2022a), and 1 December to 19 January (2022-2023; Portela et al., 2025). All gliders were deployed from the fast ice near Ross Island (where calibration casts were not feasible) and recovered from the *RVIB* Nathaniel B. Palmer. For all three deployments, 93-95% of all dives occurred within a 1º latitude by 1º longitude box of each mean survey location. Gliders were equipped with a Seabird CT sail (accuracy within 3.01 x 10^{-4} S m^{-1}, 0.001 ºC, and 0.015% for conductivity, temperature, and pressure, respectively; seabird.com), an Aanderaa 4330F oxygen optode (accuracy of ~1.5%; aanderaa.com), and a WetLabs ECO Triplet Puck (0.2-03%; Salaun and Le Menn, 2023). Sensitivities for conductivity, temperature, pressure, oxygen, backscatter, and fluorescence were 4.0 x 10^{-5} S m^{-1}, 2.0 x 10^{-4} ºC, 0.001%, 3.2 µg L^{-1}, and 0.28 ppb $count^{-1}$, and 0.025 µg L^{-1}, respectively (seabird.com, aanderaa.com).

Deleted:

Deleted: bodc.ac.uk

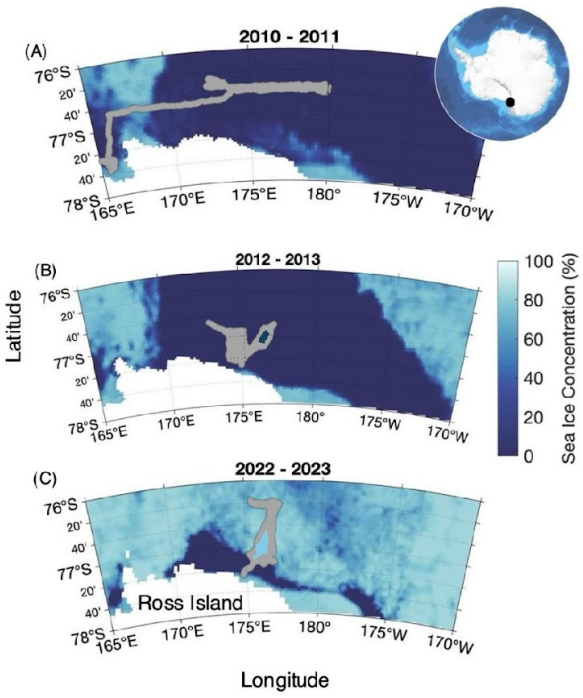

Figure 1. Maps of glider tracks from the 2010-2011, 2012-2013, and 2022-2023 deployments overlaid onto average sea ice concentrations from Dec. 1 of each year. Sea ice data comes from the University of Bremen, and the inset map of Antarctica comes from Bedmap2. The white region indicates land, and the black dot indicates the location of Ross Island.

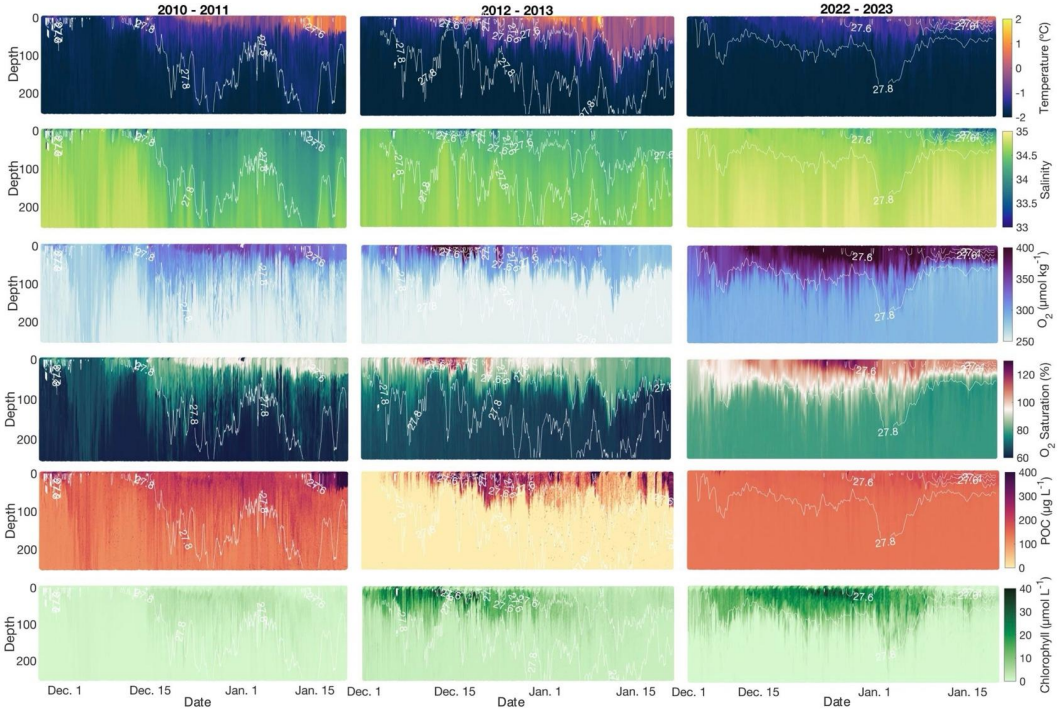

Figure 2. 2010-2011, 2012-2013, and 2022-2023 glider profiles of temperature (°C), salinity, dissolved oxygen (µmol kg^{-1}), particulate organic carbon concentrations (POC; µg C L^{-1}), and chlorophyll (µg L^{-1}) by date. Contours represent isopycnals. All profiles are for the upper 250 m.

CTD calibration casts were conducted by scientists aboard the *RVIB* Palmer in the near vicinity (<400 m from the glider's location) coincident with glider recovery. Discrete samples were collected for chlorophyll *a* and POC. Chlorophyll *a* samples were analysed fluorometrically on ship whereas POC samples were stored and analysed onshore via an elemental analyser at the Virginia Institute of Marine Science (Gardner et al., 2000). Discrete chlorophyll *a* samples were used to convert glider fluorometer voltages to optically-based chlorophyll, and discrete POC samples were used to convert optical backscatter counts at 470 nm wavelength ($b_{bp}(470)$) to POC according to the method of Boss and Pegau (2011). For both chlorophyll and POC samples, single equations converting fluorescence to chlorophyll and backscatter to POC were individually generated per year (Fig. S1). Dissolved oxygen sensors were factory calibrated and compared with profiles collected from the CTD rosette (R^2 = 0.89, 0.76, and 0.96 for 2010-2011, 2012-2013, and 2022-2023, respectively). A full discussion of sensors, discrete samples, and calibrations is provided by Kaufman et al. (2014), Queste et al. (2015), Meyer et al. (2022a), and Portela et al. (2025).

Deleted:

2.2 Biogeochemical Rate Measurements

Three biogeochemical rates were calculated per deployment: NCP, $\frac{\partial POC}{\partial t}$, and $Export^{*}_{POC}$. Rates were calculated for non-overlapping, consecutive three-day intervals over the duration of each deployment. To make the time period of analysis comparable between deployments, they were trimmed to only include days where euphotic zone (Z_{eu}) averaged chlorophyll concentrations were within 90% of the peak chlorophyll concentration (Fig. S2). Z_{eu} was calculated as 1% of maximum measured photosynthetic active radiation (PAR) when PAR was available (2022-2023) or according to Morel (1974) when PAR was unavailable (2010-2011, 2012-2013). NCP was calculated via a mass balance of glider-based dissolved oxygen concentrations via Equation 1:

$$NCP_{100} = PQ * (\int_0^{100} \frac{\partial O_2}{\partial t} - F_{K_z} - F_{Adv} - ASE_{ML}) \quad \text{(Eq. 1)}$$

Deleted: $\frac{\partial O_2}{\partial t}$

where PQ is photosynthetic quotient (i.e., the molar ratio of oxygen to carbon produced during photosynthesis), $\int_0^{100} \frac{\partial O_2}{\partial t}$ is the change in O_2 concentrations integrated over the top 100 m from the beginning of day 1 to the end of day 3 of each 3-day

period. 100 m is a common reference depth at which to assess carbon export efficiency, and thus was chosen as our depth threshold (Buesseler et al., 2020). F_{K_z} is the vertical eddy diffusion flux of oxygen to the water below 100 m, using the previously published vertical diffusivity coefficient (K_z) of 10^{-3} m^2 s^{-1} for the Ross Sea (Kaufman et al., 2017). F_{Adv} is the advective flux of oxygen in the zonal and meridional directions with velocity calculated according to dive average currents (DAC) obtained from fitting a hydrodynamic model to the glider's flight path (Frajka-Williams et al., 2011). Because our glider surveys were not grids and thus limited our ability to generate individual x-y gradients, deployment-wide average DACs and zonal and meridional gradients of oxygen were used to calculate 3-day advection rates (F_{Adv}) for each 3 m depth bin (Fig. S3). Individual F_{Adv} for each 3 m bin were then depth-integrated over 100 m to derive a value for each deployment according to Equation 2:

$$F_{ADV} = \int_0^{100} \left(u * \frac{\partial O_2}{\partial x} + v * \frac{\partial O_2}{\partial y}\right) \quad \text{(Eq. 2)}$$

where ASE_{ML} is air-sea exchange of oxygen between the atmosphere and the surface mixed layer. Mixed layer depths were calculated according to potential density difference threshold of 0.02 kg m^{-3} from potential densities at 10 m. Air-sea exchange was calculated according to the bubble injection method outlined by Liang et al. (2013). Daily wind speed (m s^{-1}) and sea surface pressure (pascals) data come from the National Center for Environmental Prediction (NCEP) Reanalysis 1 product (2.5º x 2.5º resolution; Kalnay et al., 1996; Fig. 3E; Fig. 3G), which has been shown to be more accurate than ECMWF Reanalysis data in this region (Sanz Rodrigo et al., 2012; Fig. S4). The gas transfer velocity coefficient from Wanninkhof (2014) and the polar specific photosynthetic quotient (1.3) from Laws (1991) were used. During the bloom period, we assume entrainment flux, lateral mixing, and vertical advection at the 100 m boundary to all be minimal and are thus omitted. NCP data are presented in units of g C m^{-2} d^{-1} with positive values indicating net autotrophy (photosynthesis outpacing respiration) and negative values indicating net heterotrophy (respiration outpacing photosynthesis).

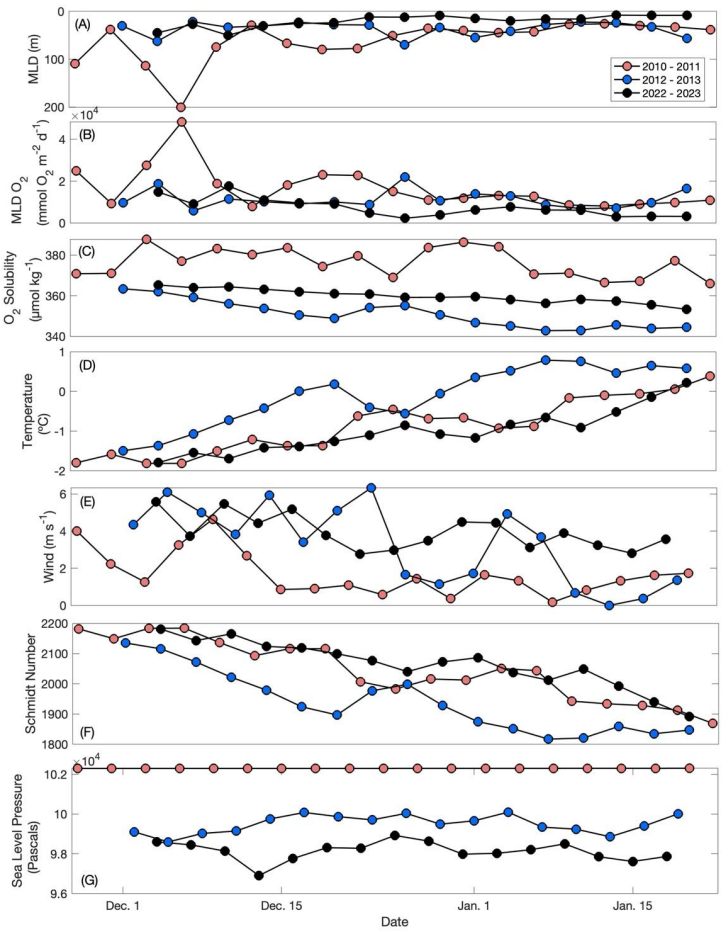

Figure 3. Mixed layer depth (A; m), mixed layer integrated dissolved oxygen (B; mmol O_2 m^{-2} d^{-1}), oxygen solubility (C; µmol O_2 kg^{-1}), temperature (D; ºC), wind (E; m s^{-1}), Schmidt number (F), and sea level pressure (G; pascals) through time for the 2010-2011, 2012-2013, and 2022-2023 deployments. Schmidt number calculations come from Wanninkhof (2014), and wind and sea level pressure are NCEP Reanalysis products. All other parameters come from glider measurements.

$\frac{\partial POC}{\partial t}$ was calculated according to Equation 3:

$$\frac{\partial POC}{\partial t} = \int_0^z \frac{\partial POC}{\partial t} - F_{ADV} \quad \text{(Eq. 3)}$$

where $\int_0^z \frac{\partial POC}{\partial t}$ is the change in integrated POC concentration between days 1 and 3, and F_{Adv} is the advective flux of POC derived in the same manner as for oxygen. During the 2012-2013 deployment, the backscatter sensor was turned off below 250 m to save battery power (Jones and Smith, 2017; Meyer et al., 2022a). Therefore, all deployments were analysed for changes in POC to a 240 m depth threshold (Z = 240 m) to maintain consistency between datasets.

Integrated concentrations of both carbon and oxygen are sensitive to the choice of integration depths of 240 m and 100 m respectively. Mixed layer depths had ranges of 26 – 201 m, 22 – 70 m, and 9 – 70 m, for 2010 - 2011, 2012 - 2013, and 2022 - 2023, respectively (Fig. 3A). During analysis, multiple integration depths of both dissolved oxygen and POC were tested. In 2010 – 2011, 2012 – 2013, and 2022 – 2023, O_2 concentrations integrated to 100 m were 64, 39, and 70% higher than mixed layer integrated values, respectively. POC concentrations integrated to 500 m were 64 and 49% higher than the 240 m integrated values for 2010 – 2011 and 2022 -2023, respectively. Therefore, consistent integration depths should be applied across datasets. While 100 m is a common integration depth for production metrics in production-export analyses, ideally POC addition and removal should be evaluated as deep as the dataset allows in order to generate a carbon export rate most similar to carbon sequestration rates (typically defined as carbon export to 1000 m; Boyd et al., 2019). Here, a negative $\frac{\partial POC}{\partial t}$ denotes a removal (i.e., a decrease in POC concentrations through time) whereas a positive $\frac{\partial POC}{\partial t}$ denotes an increase of POC concentrations through time.

POC export potential is the amount of POC available for export in the upper 200 m at the end of the study period. Because each deployment ended before the final bloom succession and biomass export, we measure a potential, rather than actualized export at the end of the deployment period (Hansell and Carlson, 1998; Sweeney et al., 2000). Here, POC export potential was estimated as the difference between the two rates:

$$Export^*_{POC} = NCP - \frac{\partial POC}{\partial t} \quad \text{(Eq. 4)}$$

Deleted: values

Deleted: Add here the same sentence but stating the euphotic depths, so we have the context for these depths.

Deleted:

Deleted: 78

Deleted: with mixed layer depths ranging from 26 – 201 m, 22 – 70 m, and 9 – 70 m for 2010 - 2011, 2012 - 2013, and 2022 - 2023, respectively

Deleted: 51

Deleted:

Deleted: positive

Deleted: negative

Equation 4 represents a difference from the calculation of POC export due to the non-steady state nature of the spring bloom period (Cassar et al., 2015). NCP and $\frac{\partial POC}{\partial t}$ are integrated over different depth thresholds in accordance with practices established by the Martin curve which assesses export in between 100 m and a variable depth Z (Martin et al., 1987).

The percent standard deviation of stocks and rates were assessed by calculating the percent standard deviation of O_2, POC, $\frac{\partial O_2}{\partial t}$, and $\frac{\partial POC}{\partial t}$ per season according to Equation 5:

$$\%\ \text{Standard Deviation} = \left(\frac{Standard\ Deviation}{Mean}\right) * 100 \quad \text{(Eq. 5)}$$

2.3 Uncertainties

One source of uncertainty in our analysis arises from the estimates of advection. In each deployment, the gliders surveyed in various patterns, making repeat observations of the same water masses and thus quantification of POC and O_2 gradients and currents difficult. However, given these surveys occurred during the Ross Sea bloom period, temporal changes are a first order control on observations and spatial changes are a secondary control. This is supported by very low rates of F_{ADV} and spatiotemporal comparison of observations between multiple gliders in 2022-2023 (Fig. S5). Values of F_{ADV} may also be influenced by the use of DACs averaged over the entire dive rather than the upper 100 m, but given the low F_{ADV} values relative to NCP, this does not make a substantial difference in the calculation. For example, if supposed F_{ADV} is underestimated by 50%, this only leads to an underestimate of 0.3, 0.7, and 4.0 mg C m^{-2} d^{-1} in our calculations for 2010 – 2011, 2012 – 2013, and 2022 – 2023, respectively.

Our analysis hinges on the assumption that bio-optical proxies represent their assumed biogeochemical parameter accurately. Because POC and chlorophyll *a* concentrations were validated in situ, this assumption is valid. Oxygen concentrations were only factory calibrated and thus likely include higher uncertainty (Bittig et al., 2018). Propagation of uncertainty for all biogeochemical rate measurements was calculated following the method of Yang et al. (2017). We used the offset (i.e., the y-intercept) between glider and CTD oxygen optodes and fluorometers to calculate the uncertainty associated with oxygen and POC concentrations (Fig. S1). For the K_z and Schmidt number, we used the previously reported uncertainties of ±7-10% from Yang et al. (2017). This led to mean NCP uncertainties ranging from ±76% to ±94%, $\frac{\partial POC}{\partial t}$ uncertainties ranging from ±38% to ±45%, and $Export^{*}_{POC}$ uncertainties ranging from ±47% to ±61% across each season.

Formatted: Subscript

Formatted: Centred

Formatted: Subscript

Formatted: Superscript

Formatted: Superscript

Deleted: . The average oxygen offsets were ±78%, ±95%, and ±76% of CTD values, and the average POC offsets were ±45%, ±66%, and ±32% of CTD values for 2010-2011, 2012-2013, and 2022-2023, respectively

Deleted:

3 Results

3.1 Net Community Production

Rates of NCP in 2022-2023 were highly variable but suggest net autotrophy with a deployment-wide mean (± standard deviation of all 3-day periods) of 0.2 ± 3.2 g C m^{-2} d^{-1} (Fig. 4A). This value is highest of the three deployments- higher than the mean of -0.7 ± 4.6 g C m^{-2} d^{-1} in 2012-2013 and somewhat higher than the 2010-2011 deployment mean of 0.1 ± 3.8 g C m^{-2} d^{-1} (Fig. 4A). The 2022-2023 season was highly variable, consistent with previous deployments (Fig. 4A). Additionally, the magnitudes of NCP in each deployment were high with approximately half (50%, 48% and 63% for 2010-2011, 2012-2013, and 2022-2023, respectively) of NCP 3-day rates greater than 1.5 g C m^{-2} d^{-1} or less than -1.5 g C m^{-2} d^{-1}. The 2010-2011 season exhibited the single greatest productivity event in mid-December when NCP, driven by $\frac{\partial O_2}{\partial t}$, reached 13.0 g C m^{-2} d^{-1} (Fig. 4A). This one 3-day period increased the seasonal average by 0.6 g C m^{-2} d^{-1}, moving it from slightly heterotrophic (-0.5 g C m^{-2} d^{-1}) to solidly autotrophic. In all three deployments, NCP was driven by $\frac{\partial O_2}{\partial t}$, reinforcing the notion that biology is the largest driver of changes in upper ocean oxygen content during the bloom period, evidenced by this term being an order of magnitude greater than any of the other terms in the oxygen budget (Fig. 5A; Fig. 6; Fig. S6; Fig. S7). Despite the substantial

temporal variability between the 3-day periods and negative average NCP observed in 2012-2013, our findings suggest that the Ross Sea is capable of high rates of production during the spring bloom period.

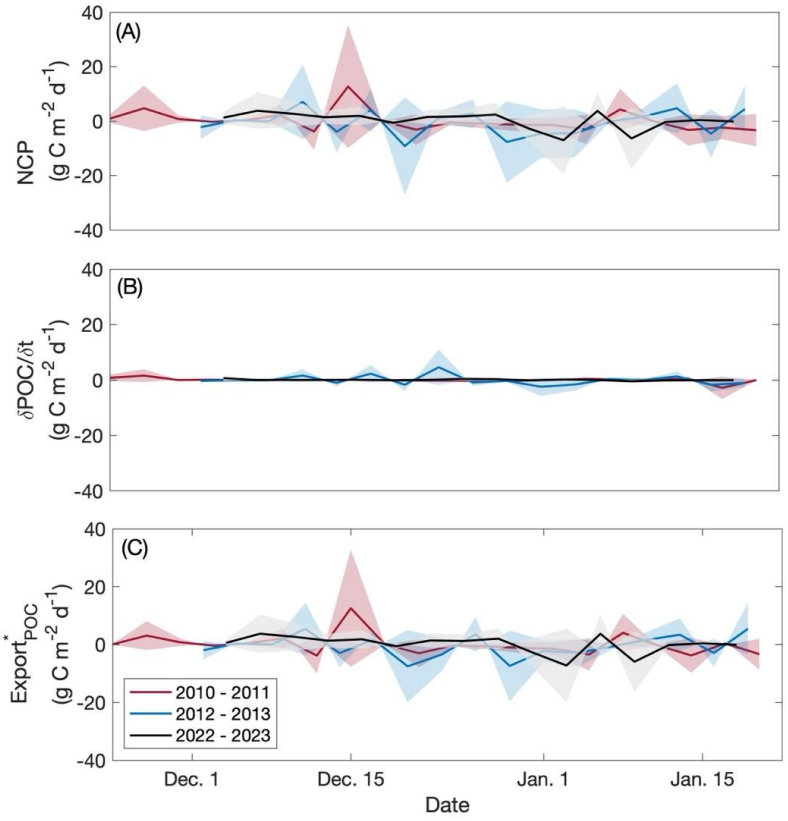

Figure 4. Net community production (A), $\frac{\partial POC}{\partial t}$ (B), and $Export^{*}_{POC}$ (C) through time for glider deployments occurring in the 2010-2011, 2012-2013, and 2022-2023 productive seasons. Units for all rates are g C m^{-2} d^{-1}. Shaded regions represent uncertainty for each rate. For NCP, positive values indicate autotrophy, and negative values indicate heterotrophy. For $\frac{\partial POC}{\partial t}$, positive indicates an increase in POC through time whereas negative indicates a decrease.

Deleted: decrease

Deleted: n

Deleted: increase

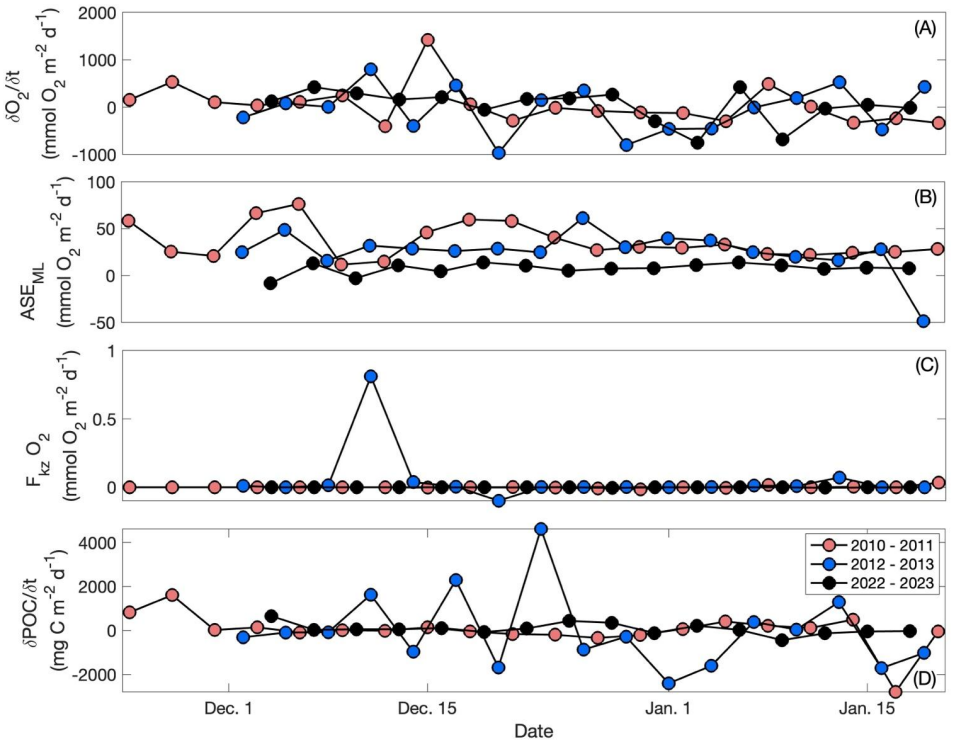

Figure 5. $\frac{\partial O_2}{\partial t}$ **(A; mmol O₂ m⁻² d⁻¹), ASE$_{ML}$ (B; mmol O₂ m⁻² d⁻¹), F$_{Kz}$ O₂ (C; mmol O₂ m⁻² d⁻¹), and** $\frac{\partial POC}{\partial t}$ **(D; mg C m⁻² d⁻¹) by day for the 2010-2011, 2012-2013, and 2022-2023 glider deployments. Note different scales between the y-axes.**

The individual components of NCP (particularly, $\frac{\partial O_2}{\partial t}$ and ASE$_{ML}$) varied substantially between years (Fig. 5). Due to the bloom, $\frac{\partial O_2}{\partial t}$ was the largest component in each year with the highest average rate occurring in 2010-2011 (48 ± 410 mmol O_2 m^{-2} d^{-1}; Fig. 5A). ASE$_{ML}$ was greatest (36 ± 18 mmol O_2 m^{-2} d^{-1}) in 2010-2011, consistent with the deepest mixed layers during this year, suggesting that stronger winds that year are responsible for both (Fig. 4B; Fig. 5E). ASE$_{ML}$ was likewise large

(26 ± 22 mmol O_2 m^{-2} d^{-1}) in 2012-2013 when winds were strong (Fig. 3E; Fig. 5B; Meyer et al., 2022a). In all deployments, F_{kz} made a negligible contribution to total NCP (<0.01 – 0.1%; Fig. 5C; Fig. 5D). F_{ADV} was also low with deployment-wide averages of 7.3 x 10^{-3}, -0.1, and 1.4 mmol O_2 m^{-2} d^{-1} for 2010-2011, 2012-2013, and 2022-2023, respectively.

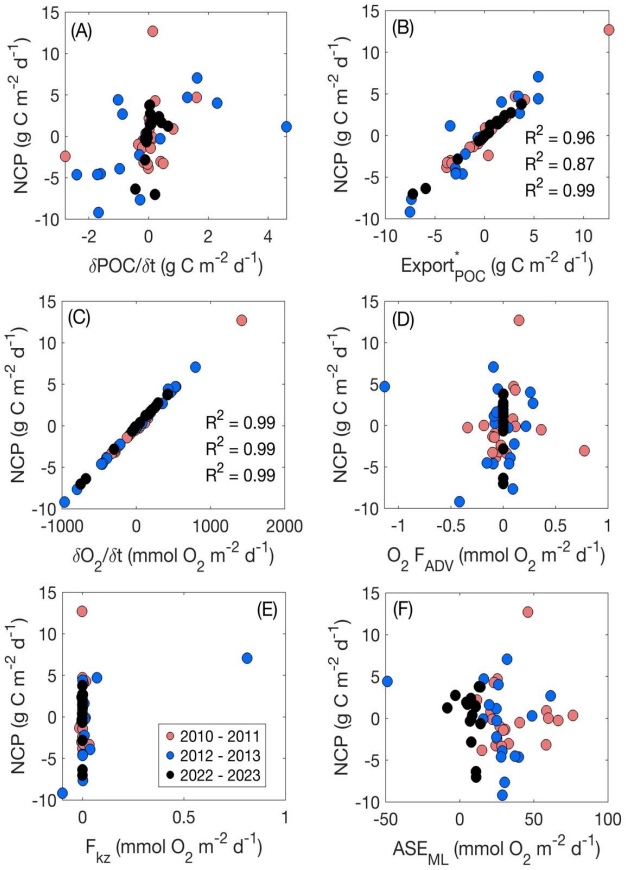

Figure 6. Net community production (NCP; g C m^{-2} d^{-1}) versus biogeochemical rates ($\frac{\partial POC}{\partial t}$, $Export^{*}_{POC}$; g C m^{-2} d^{-1}) and components of NCP ($\frac{\partial O_2}{\partial t}$, O_2 F_{ADV}, F_{Kz}, and ASE_{ML}; mmol O_2 m^{-2} d^{-1}) per day for 2010-2011, 2012-2013, and 2022-2023 glider deployments. R^2 values indicate correlation coefficients.

3.2 Changes in POC through time

$\frac{\partial POC}{\partial t}$ and the relationship between $\frac{\partial POC}{\partial t}$ and NCP behaved differently among deployments (Fig. 5; Fig. 6). $\frac{\partial POC}{\partial t}$ was highest in 2022-2023 when NCP was likewise highest, but POC concentrations were lower during this season than in 2012-2013 (Meyer et al., 2022a; Portela et al., 2025; Fig. 2). The mean 2012-2013 $\frac{\partial POC}{\partial t}$ rate was similar in magnitude (-0.05 ± 1.7 g C m^{-2} d^{-1}) to that of 2022-2023 despite 2012-2013 having a substantially lower NCP rate than in 2022-2023 (Fig. 4B). Like with oxygen, advection of POC was negligible across seasons (averages were 4.3 x 10^{-3}, -0.4, and 4.3 mg C m^{-2} d^{-1} for 2010-2011, 2012-2013, and 2022-2023, respectively) and thus, did not contribute substantially to calculations of $\frac{\partial POC}{\partial t}$ (Fig. 5F). Compared with NCP, rates of $\frac{\partial POC}{\partial t}$ per season were all low, suggesting that during the observation period, high rates of production are not matched by high rates of POC removal.

3.3 POC Export Potential

The temporal variability in $Export^{*}_{POC}$ is largely driven by the 3-day temporal variability in NCP (Fig. 4C). Thus, as expected, $Export^{*}_{POC}$ rates were highest in 2022-2023 (0.2 ± 3.1 g C m^{-2} d^{-1}) and lowest in 2012-2013 (-0.6 ± 3.9 g C m^{-2} d^{-1}). In 2023, $Export^{*}_{POC}$ from 1 to 3 January was one of the lowest in magnitude observed across all three deployments at -7.2 g C m^{-2} d^{-1} (Fig. 4C). This value was driven by negative NCP and suggests substantial rates of loss processes. Due to its low mean $\frac{\partial POC}{\partial t}$, $Export^{*}_{POC}$ in 2010-2011 (0.1 ± 3.7 g C m^{-2} d^{-1}) was comparable to NCP, reinforcing the idea of biomass accumulation in the surface ocean through time during this season. $Export^{*}_{POC}$ was also greater than NCP in 2012-2013 but is driven by a variable, frequently negative NCP with biomass accumulation during the observation period, leading to negative average NCP, $\frac{\partial POC}{\partial t}$, and $Export^{*}_{POC}$. Like NCP, our average $Export^{*}_{POC}$ is quite high, comparable to 68-100% of the total NCP on average. This finding suggests that substantial POC exists within the top 240 m of the water column but is not being removed (e.g., through sinking, grazing, remineralization, etc.) during our observation period.

Deleted: both

Deleted: as well as a positive $\frac{\partial POC}{\partial t}$

Deleted: negative

3.4 Stock and Rate Variability

As is evident by the large standard deviations on all 3-day means of stocks (O_2, POC) and rates (NCP, $\frac{\partial POC}{\partial t}$), variability appears to be an important consideration when assessing potential drivers and temporal differences between the parameters of interest. Because the glider and water masses are both moving, the variability evaluated here represents both seasonal spatial and temporal variability of stocks and rates. When evaluated seasonally, spatial variability will be averaged over and temporal variability is likely to be dominant due to the evolution of the bloom (Fig. S5). Substantial variability of POC and O_2 concentrations themselves is not diagnostic of substantial variability in rate patterns. However, an inverse relationship is apparent between variability, in the form of percent standard deviation, of $\frac{\partial O_2}{\partial t}$ and NCP. The highest magnitude of percent standard deviation (-1.1 x 10^3%) coincides with lowest NCP in 2012-2013, and lowest magnitude of percent standard deviation (780%) coincides with highest NCP in 2022-2023 (Fig. 7).

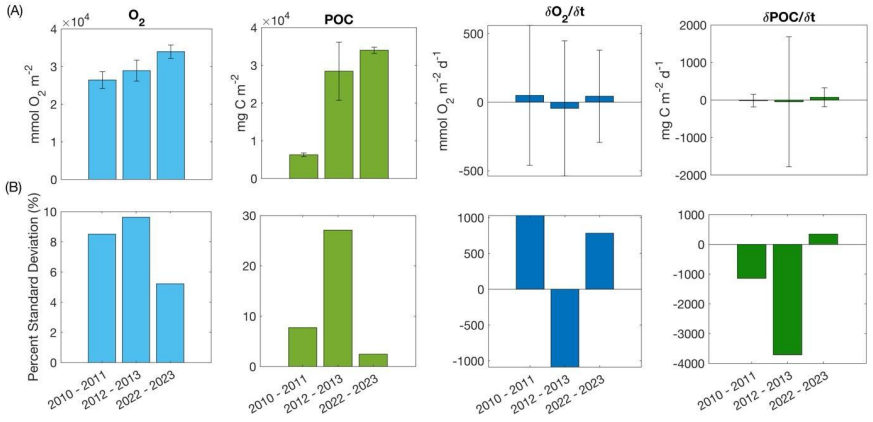

Figure 7. Averages and standard deviations (A) and percent standard deviations (B; all units are %) for dissolved oxygen (mmol O_2 m^{-2}), particulate organic carbon (POC; mg C m^{-2}), $\frac{\partial O_2}{\partial t}$ (mmol O_2 m^{-2} d^{-1}) and $\frac{\partial POC}{\partial t}$ (mg C m^{-2} d^{-1}) for the 2010-2011, 2012-2013, and 2022-2023 deployments.

The variability analysis also highlights some key discrepancies between the mean concentration of parameters between years versus changes through each season and how these relate to the biogeochemical rates of interest (Fig. 7). The time-mean of depth-integrated dissolved oxygen concentrations and POC concentrations exhibited different patterns relative to $\frac{\partial O_2}{\partial t}$ and $\frac{\partial POC}{\partial t}$ (i.e., years with the highest or lowest dissolved oxygen or POC concentrations did not correspond to years with the highest $\frac{\partial O_2}{\partial t}$ or $\frac{POC}{\partial t}$). Highest mean integrated dissolved oxygen concentrations ($3.4 \times 10^4 \pm 1.8 \times 10^3$ mmol O_2 m^{-2} d^{-1}) were observed in 2022-2023 when $\frac{\partial O_2}{\partial t}$ and NCP were highest, but 2012-2013 had higher average oxygen concentrations but a much lower NCP than 2010-2011 (Fig. 2; Fig. 4A). Differing patterns were also evident when comparing POC concentrations and $\frac{\partial POC}{\partial t}$. However, discrete dissolved oxygen and POC exhibited the highest concentrations in 2012-2013 (Fig. 2). The lower-than-average POC concentrations in 2022-2023 are particularly obvious when evaluated as the mean of concentrations at discrete depths (Fig. 8). The increase in difference (to approximately 20%) between 25 m and 50 m average concentrations toward mid-January would suggest that POC is being retained above 50 m. Unlike POC, chlorophyll concentrations were much higher in 2022-2023 than the other two years (Fig. 2).

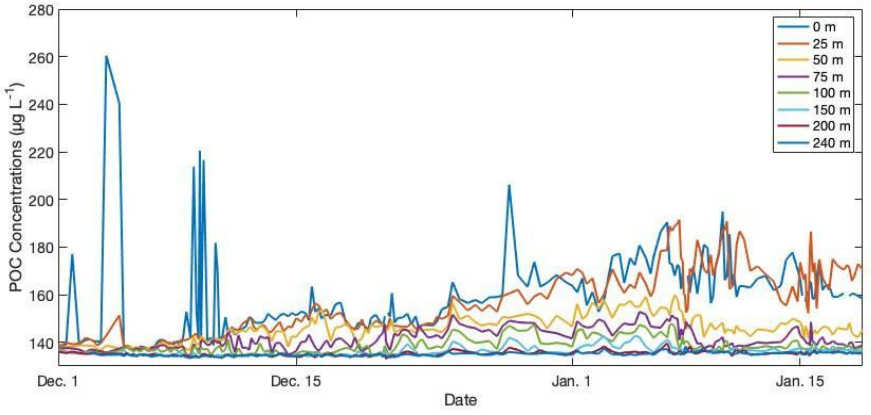

Figure 8. Average particulate organic carbon concentrations (µg C L^{-1}) per depth of interest through time from the 2022-2023 glider deployment. Depths of interest include 0, 25, 50, 75, 100, 150, 200, and 240 m.

4 Discussion

The ability to resolve the surface O_2 and POC fluxes defining these biogeochemical rates at very high spatiotemporal resolution over multiple years provides a better understanding of biological vs. physical controls on the system during the spring bloom. Fig. 6 highlights the consistently strong, positive relationship between NCP, $\frac{\partial O_2}{\partial t}$, and $Export^*_{POC}$ during all deployments. Despite varying rates of O_2 F_{ADV}, F_{Kz}, and ASE_{ML} between deployments , $\frac{\partial O_2}{\partial t}$ is always the dominant term in the upper ocean dissolved oxygen budget, determining trends in NCP which in turn, determine trends in $Export^*_{POC}$ (Fig. 4; Fig. 5). Likewise, $\frac{\partial POC}{\partial t}$ appears consistently uncoupled from NCP (Fig 6). These findings suggest that, despite substantially varying hydrographic and biogeochemical attributes between seasons, a consistent relationship between production-export dynamics exists between seasons. Thus, our results support the classification of the Ross Sea as a high production, low export system (Henson et al., 2019), but the high-resolution data provided by the gliders show substantial 3-day temporal variability during the bloom season that is likely a consistent, yet overlooked, feature of this system. Our results show that this temporal variability impacts rates and our understanding of the relationship between rates when investigated on the sub-seasonal level.

Our results show that biogeochemical rates and stocks appear uncoupled, with no apparent, strong relationship between NCP and $\frac{\partial POC}{\partial t}$ rates per season. Seasonal mean NCP varied substantially between years, but seasonal mean $\frac{\partial POC}{\partial t}$ did not, with the three years all within approximately 0.3 g C m^{-2} d^{-1} of each other. This suggests that the variable environmental and biological conditions that lead to substantial differences in NCP are not as strong a control on $\frac{\partial POC}{\partial t}$ as they are for NCP. Thus, a higher NCP does not necessarily translate to higher $\frac{\partial POC}{\partial t}$. For example, the low rates of $\frac{\partial POC}{\partial t}$ in the 2010-2011 season likely stem from the low POC concentrations (Fig. 3) and a variable mixed layer depth, which could prevent substantial POC accumulation due to mixing induced light limitation, (Fig. 2A) during this period. Therefore, $\frac{\partial POC}{\partial t}$ must be kept relatively low by some external factor that was not measured during this study, such as differing lability of *P. antarctica* versus diatoms (or lack thereof; Misic et al., 2017; Misic et al., 2024) and the role of particle-attached bacteria and remineralization (Becquevort

Formatted: Font: Italic

and Smith, 2001) on backscatter measurements and remains relatively invariant. Coupling glider studies with such analyses should be conducted in future studies as they may help elucidate the mechanism behind consistent $\frac{\partial POC}{\partial t}$ between seasons.

The ratio of $\frac{\partial POC}{\partial t}$ to NCP can be considered a proportional POC removal (i.e., how much of the POC that was produced by the bloom during the observation period is removed during the observation period; Fig. 9). The implications of this proportional removal are important for evaluating a system's production-export efficiency. Our results suggest that the proportion of POC removed (Fig. 9) is more important for carbon cycling at times when there is either high NCP and high biomass accumulation as in 2022-2023 or low NCP but high biomass as in 2012-2013, rather than times where there is high NCP but lower biomass as in 2010-2011.

The 2012-2013 glider observations extended into February, approximately two weeks longer than the other deployments. When late January and early February rates are included, and values averaged over the entire deployment, NCP is low at 0.05 ± 2.75 whereas $\frac{\partial POC}{\partial t}$ is much higher at 0.23 ± 1.24 g C m^{-2} d^{-1} (Meyer et al., 2022a). Additionally, these rates were calculated in 5-day intervals, not 3, so some sub-seasonal variability is likely being smoothed and overlooked due to the longer integration period. This difference in average rates further supports the notion that, due to substantial temporal variability, the timescales over which these rates are averaged is critically important if we want to detect signals of climate change. Thus, establishing our evaluation timeframe based on an ecological, rather than temporal, metric (such as chlorophyll concentration) is important and should lead to more biogeochemically-reflective rate estimates. These rates are important to

Deleted: Albeit

Deleted: we would argue that calculating these biogeochemical rates on <5-day timescales should lead to more accurate rate estimates and …

compare over the time period when chlorophyll concentrations are greater than 10% of peak bloom concentrations regardless of the exact days of year.

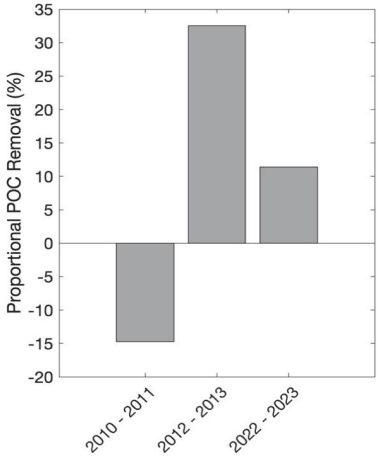

Figure 9. Deployment average proportional POC removal (%; i.e., $\frac{\partial POC}{\partial t}$ / NCP) per season. Negative values reflect a decoupling of accumulation and removal processes over the course of our study.

This notion of uncoupling between production and export processes is supported by the high retention of POC in the upper water column in 2022-2023 (Fig. 8). Biomass retention is evident by the increasing difference between the mean daily POC concentrations at 25 vs. at 50 m (i.e., POC concentrations at 25 m are up to ~20% higher than 50 m) from the beginning to the end of the deployment (Fig 8). Biomass retention is also supported by greater integrated POC concentrations in 2022-2023 (34.0 g C m^{-2}) than in 2012-2013 when concentrations declined more from surface to depth (28.4 g C m^{-2}; Fig. 2). Some of this difference between years may be taxonomically driven as different phytoplankton groups possess different concentrations of cellular carbon (Rousseau et al., 1990; Smith and Kaufman, 2018), but the daily averaged C:Chl ratios at 5 m, representing the typical surface values, for 2012-2013 and 2022-2023 both increased in late December - early January (Fig. S8). The limited availability of POC and Chl calibration samples prevent us from resolving any specific POC and Chl concentration differences between phytoplankton groups which may lead to slight under- or overestimations of POC, Chl, and

Deleted: evaluate

Deleted: Fig. S6

Deleted: will not

Deleted: e

C:Chl ratios as the bloom evolves. Despite this, the dramatic change in C:Chl ratios through time is typical of the annual bloom and suggests a mixed community with a shift from *Phaeocystis* to diatom dominance over time (Jones and Smith, 2017; Smith and Kaufman, 2018).

Our NCP, $\frac{\partial POC}{\partial t}$, and $Export^{*}_{POC}$ time series (Fig. 4) reinforce the influence of short-term temporal variability, on the order of days, on seasonal means. This is further emphasised when comparing the 2010-2011 dataset evaluated in this study with a previously published study with a different methodology (Queste et al., 2015). In their study, Queste et al. calculated daily oxygen changes as the linear regression of apparent oxygen utilisation against time at various depth bins. When evaluating the same period, they found NCP rates ranging from -0.9 to 0.7 g C m^{-2} d^{-1} (Queste et al., 2015). When averaged over the entire deployment, NCP in 2010-2011 from this current study is autotrophic but highly variable at 0.1 ± 3.8 g C m^{-2} d^{-1} (Fig 4A). This can be attributed to the period from 13 to 15 December, which due to differences in integration periods for the calculations, appears to be smoothed in the results of Queste et al. but more apparent in our study. During this period, NCP is 13.0 g C m^{-2} d^{-1} resulting from an exceptionally high $\frac{\partial O_2}{\partial t}$ (1420 mmol O_2 m^{-2} d^{-1}; Fig. 5A) but moderate F_{ADV}, F_{Kz}, and ASE_{ML} (0.15, 46, -1.9 x 10^{-3} mmol O_2 m^{-2} d^{-1}, respectively). Oxygen concentrations themselves during this time do not appear anomalous (i.e., all dives on 13 to 15 Dec. are internally consistent and within the range observed during 2010-2011), suggesting that this is a real signal with a dramatic (>4.27 x 10^{3} mmol O_2 m^{-2}) increase over a short period of time (Fig. 5A). Additionally, the oxygen concentrations immediately before 13 Dec were not anomalously low. Removing the mid-December peak in NCP decreases the 2010-2011 average, making the values similar to those found by Queste et al. (2015). The importance of a singular event to the average 2010-2011 NCP may help explain the substantially lower $\frac{\partial POC}{\partial t}$ during this season compared with the other two seasons, i.e., a short event does not have as strong an influence in increasing net POC as a consistent period of high NCP. This is likely due to the highly productive nature of the Ross Sea. Other studies have found that in regions of lower average primary production, short-term events have greater net impacts on primary production and/or export (Meyer et al., 2022b). Our study reinforces the influence that integration periods have on results, particularly when analysing NCP during highly dynamic periods (see Niebergall et al. (2023) for a discussion of the role of integration time and space on NCP).

The high NCP observed in 2022-2023 coincides with higher than average chlorophyll *a* concentrations and a stable water column (Fig 2; Portela et al., 2025). While surface POC concentrations are lower than the average typically reported for

Deleted: out

Deleted:

Deleted:

Deleted: importance of using short

the Ross Sea bloom period (Smith and Kaufman, 2018; Meyer et al., 2022a), depth-integrated POC was high, indicating a substantial accumulation of biomass and retention of that biomass during this season. Portela et al. (2025) provide a more complete discussion of the characteristics and potential drivers of this larger-than-average bloom. The overall characteristics of the 2022-2023 season sharply contrast with the more dynamic, lower biomass (in terms of both chlorophyll and POC), low $\frac{\partial POC}{\partial t}$ 2010-2011 season. Portela et al. (2025) note substantial differences in Ross Sea sea ice concentration, as is evident in Fig. 1, between these two years with 2022-2023 having more ice and a later opening of the polynya than 2010-2011 and cite this as a possible mechanism leading to the high chlorophyll concentrations observed in 2022-2023. The influence of sea ice concentration on production through iron seeding, water column stabilisation, and enhanced mixing has been highlighted previously (Arrigo et al., 2008; Smith and Comiso, 2008; Queste et al., 2015).

Current ecosystem models predict that due to alleviation of light limitation, increases in iron concentration, and warmer temperatures, primary production and phytoplankton biomass in the Southern Ocean generally may increase (Moreau et al., 2015; Ferreira et al., 2024). Trends in Ross Sea sea ice cover have varied substantially over the last few decades, showing changes which are frequently masked in compilations of the entire Southern Ocean (Turner et al., 2022). This makes accurate projections of the direction and magnitude of change for future Ross Sea ice cover difficult. Contrary to some studies, our findings suggest that heavy ice cover may, at least temporarily, increase rates of primary production and phytoplankton biomass (Portela et al., 2025). Alternatively, some studies suggest that reduced ice cover will increase long term primary production due to the alleviation of light limitation, warmer temperatures, and increased nutrient availability (Thomalla et al., 2023). Regardless, our study suggests that an increase or decrease in primary production and POC concentrations in coming decades does not necessarily induce substantial changes in carbon export in the Ross Sea. More research is needed to fully elucidate the fate of POC in the late bloom season in the Ross Sea.

5 Conclusion

When compared with global averages, high-resolution data from three glider deployments support the classification of the Ross Sea as a high production, low export system. Our data highlight temporal uncoupling between biogeochemical stocks (POC, O_2) and rates (NCP, $\frac{\partial POC}{\partial t}$, $Export^{*}_{POC}$) and between related rates (NCP and $\frac{\partial POC}{\partial t}$) when evaluated on short-term (3-day)

and seasonal scales during three spring bloom periods. Much of this uncoupling relates to substantial variability which drives rates and reinforces the need for high-resolution measurements. While all three deployments warrant additional observations into the Autumn to document the bloom demise and diatom reduction, the implications for production-export dynamics during the peak productive period are clear: high NCP leads to high $Export^{*}_{POC}$ and low NCP leads to low or even negative $Export^{*}_{POC}$ regardless of the average surface POC and O_2 concentrations during the bloom. These findings should be considered when using just stock concentrations to investigate these dynamics in the Ross Sea.

Data Availability

All data presented here are publicly available at the Biological and Chemical Oceanography Data Management Office (dataset IDs 532608 and 568868) and the British Oceanographic Data Centre (Deployment ID 596). Auxiliary data utilized in figures and equations can be found at data.seaice.uni-bremen.de (sea ice concentration), and psl.noaa.gov/data/gridded/data.ncep.reanalysis.html (wind and sea level pressure).

Acknowledgements

We thank Bastien Queste, Danny Kaufman, and Randy Jones for their work generating the original datasets, and the UEA Glider group for piloting the gliders. We also thank the captains and crews of the *RV/IB Nathaniel B. Palmer* during each of the glider recovery cruises.

Competing Interests

One author is a member of the editorial board of OS.

Financial Support

We acknowledge funding for the NSFGEO-NERC collaborative project P2P: Plankton to Predators—Biophysical Controls in Antarctic Polynyas (NERC grant NE/W00755X/1supported MM, EP, KJH, and the 2022-2023 glider deployment) and National Science Foundation grant ANT-2040571 supported MM, WOS and the 2022-2023 glider deployment). The glider campaign was further supported by COMPASS: Climate-relevant Ocean Measurements and Processes on the Antarctic Continental Shelf and Slope (European Research Council, Horizon 2020: Grant 741120).

Deleted:
Deleted: rom the Natural Environment Research Council
Deleted:) which
Deleted: and
Deleted: .
Deleted: NSF
Deleted: and

References

Alkire, M.B., Lee, C., D'Asaro, E., Perry, M.J., Briggs, N., Cetinic, I., and A. Gray. Net community production and export from Seaglider measurements in the North Atlantic after the spring bloom. Journal of Geophysical Research, 119, 6121-6139. doi:10.1002/2014JC010105, 2014.

Arrigo, K.R., van Dijken, G.L., and S. Bushinsky. Primary production in the Southern Ocean, 1997–2006. Journal of Geophysical Research, 113, C08004. doi.org/10.1029/2007JC004551, 2008.

Becquevort, S., and W.O. Smith Jr. Aggregation, sedimentation and biodegradability of phytoplankton-derived material during spring in the Ross Sea, Antarctica. Deep Sea Research II, 48(19-20). doi.org/10.1016/S0967-0645(01)00084-4, 2001.

Bittig, H.C., Kortzinger, A., Neill, C., van Ooijen, E., Plant, J.N., Hahn, J., Johnson, K.S., Yang, B., and S.R. Emerson. Oxygen optode sensors: principle, characterization, calibration, and application in the ocean. Frontiers in Marine Science, 4. doi.org/10.3389/fmars.2017.00429, 2018.

Boss, E., and W.S. Pegau. Relationship of light scattering at an angle in the backward direction to the backscattering coefficient. Applied Optics, 40, 5503–5507. doi.org/10.1364/AO.40.005503, 2001.

Boyd, P.W., Claustre, H., Levy, M., Siegel, D.A., and T. Weber. Multi-faceted particle pumps drive carbon sequestration in the ocean. Nature 568, 327-335. doi:10.1038/s41586-019-1098-2, 2019.

Buesseler, K.O., Benitez-Nelson, C.R., Moran, S.B., Burd, A., Charette, M., Cochran, J.K., Coppola, L., Fisher, N.S., Fowler, S.W., Gardner, W.D., Guo, L.D., Gustafsson, O., Lamborg, C., Masque, P., Miquel, J.C., Passow, U., Santschi, P.H., Savoye, N., Stewart, G., and T. Trull. An assessment of particulate organic carbon to thorium-234 ratios in the ocean and their impact on the application of ^{234}Th as a POC flux proxy. Marine Chemistry, 100, 213-233. doi:10.1016/j.marchem.2005.10.013, 2006.

Buesseler, K.O., Boyd, P.W., Black, E.E., and D.A. Siegel. Metrics that matter for assessing the ocean biological carbon pump. Proceedings of the National Academy of Sciences, 117, 9679-9687. doi/10.1073/pnas.1918114117, 2020.

Cassar, N., Wright, S.W., Thomson, P.G., Trull, T.W., Westwood, K.J., de Salas, M., Davidson, A., Pearce, I., Davies, D.M., and R.J. Matear. The relation of mixed-layer net community production to phytoplankton community composition in the Southern Ocean. Global Biogeochemical Cycles, 29, 446-462. doi:10.1002/2014GB004936, 2015.

Chen, S., Smith, W.O., Jr., and X. Yu. Revisiting the ocean color algorithms for particulate organic carbon and chlorophyll-a concentrations in the Ross Sea. Journal of Geophysical Research, 126. doi:10.1029/2021JC017749, 2021.

Collier, R., Dymond, J., Honjo, S., Manganini, S., Francois, R., and R. Dunbar. The vertical flux of biogenic and lithogenic material in the Ross Sea: moored sediment trap observations 1996-1998. Deep-Sea Research II, 47, 3491-3520. doi.org/10.1016/S0967-0645(00)00076-X, 2000.

Demarcq, H. Trends in primary production, sea surface temperature and wind in upwelling systems (1998-2007). Progress in Oceanography, 83, 376-385. doi:10.1016/j.pocean.2009.07.022, 2009.

DeVries, T. The oceanic anthropogenic CO2 sink: Storage, air-sea fluxes, and transports over the industrial era. Global Biogeochemical Cycles, 28(7), 631-647. doi:10.1002/2013GB004739, 2014.

Eriksen, C.C., Osse, T.J., Light, R.D., Wen, T., Lehman, T.W., and P.L. Sabin. Seaglider: a long-range autonomous underwater vehicle for oceanographic research. IEEE Journal of Oceanic Engineering 26, 424-436. doi:10.1109/48.972073, 2001.

Ferreira, A., Mendes, C.R.B., Costa, R.R., Brotas, V., Tavano, V.M., Guerreiro, C.V., Secchi, E.R., and A.C. Brito. Climate change is associated with higher phytoplankton biomass and longer blooms in the West Antarctic Peninsula. Nature Communications 15. doi:10.1038/s41467-024-50381-2, 2024.

Frajka-Williams, E., Eriksen, C.C., Rhines, P.B., and R.R. Harcourt. Determining vertical water velocities from Seaglider. Journal of Atmospheric and Oceanic Technology 28, 1641-1656. doi:10.1175/2011JTECH0830.1, 2011.

Frigstad, H, Henson, SA, Hartman, SE, Omar, AM, Jeansson, E, Cole, H, Pebody, C, and R.S. Lampitt. Links between surface productivity and deep ocean particle flux at the Porcupine Abyssal Plain sustained observatory. Biogeosciences, 12, 5885-5897. https://doi.org/10.5194/bg-12-5885-2015, 2015.

Gardner, W.D., Richardson, M.J., and W.O. Smith Jr. Seasonal patterns of water column particulate organic carbon and fluxes in the Ross Sea, Antarctica. Deep-Sea Research II, 47, 3424-3449. doi.org/10.1016/S0967-0645(00)00074-6, 2000.

Gruber, N., Landschützer, P., and N.S. Lovenduski. The variable Southern Ocean carbon sink. Annual Review of Marine Sciences, 11, 159–86. doi:org/10.1146/annurev-marine-121916-063407, 2019.

Hartman, S.E., Bett, B.J., Durden, J.M., Henson, S.A., Iversen, M., Jeffreys, R.M., et al. Enduring science: Three decades of observing the Northeast Atlantic from the Porcupine Abyssal Plain Sustained Observatory (PAP-SO). Progress in Oceanography, 191. doi:10.1016/j.pocean.2020.102508, 2021.

Hartman, S.E., Larkin, K.E., Lampitt, R.S., Lankhorst, M., and D.J. Hydes. Seasonal and inter-annual biogeochemical variations in the Porcupine Abyssal Plain 2003-2005 associated with winter mixing and surface circulation. Deep Sea Research, 57, 1303-1312. doi:10.1016/j.dsr2.2010.01.007, 2010.

Henson, S., Bisson, K., Hammond, M.L., Martin, A., Mouw, C., and A. Yool. Effect of sampling bias on global estimates of ocean carbon export. Environmental Research Letters, 19. doi:10.1088/1748-9326/adle7f, 2024.

Henson, S., Le Moigne, F., and S. Geiring. Drivers of carbon export efficiency in the global ocean. Global Biogeochemical Cycles, 33, 891-903. doi.org/10.1029/2018GB006158, 2019.

Hu, C., Feng, L., Lee, Z., Franz, B.A., Bailey, S.W., Werdell, P.J., and C.W. Proctor. Improving satellite global chlorophyll a data products through algorithm refinement and data recovery. Journal of Geophysical Research, 124, 1524-1543. doir:10.1029/2019JC014941, 2019.

Jones, R.M., and W.O. Smith Jr. The influence of short-term events on the hydrographic and biological structure of the southwestern Ross Sea. Journal of Marine Systems, 166, 184-195. doi.org/10.1016/j.jmarsys.2016.09.006, 2017.

Kalnay, E., Kanamitsu, M., Kistler, R., Collins, W., Deaven, D., Gandin, L., Iredell, M., Saha, S., White, G., Woollen, J., Zhu, Y., Chelliah, M., Ebisuzaki, W., Higgins, W., Janowiak, J., Mo, K.C., Ropelewski, C., Wang, J., Leetmaa, A., Reynolds,

R., Jenne, R., and D. Joseph. The NCEP/NCAR 40-year reanalysis project. Bulletin of the American Meteorology Society, 77, 437-470, 1996.

Karl, D.M., and M.J. Church. Microbial oceanography and the Hawaii Ocean Timeseries programme. Nature Reviews Microbiology, 12, 699-713. doi:10.1038/nrmicro3333, 2014.

Kaufman, D.E., Friedrichs, M.A.M., Smith, W.O., Jr., Queste, B.Y., and K.J. Heywood. Biogeochemical variability in the southern Ross Sea as observed by a glider deployment. Deep-Sea Research I, 92, 93-106. doi.org/10.1016/j.dsr.2014.06.011, 2014.

Laws, E.A. Photosynthetic quotients, new production and net community production in the open ocean. Deep-Sea Research, 38, 143-167, 1991.

Liang, J., Deutsch, C., McWilliams, J.C., Baschek, B., Sullivan, P.P., and D. Chiba. Parameterizing bubble-mediated air-sea gas exchange and its effect on ocean ventilation. Global Biogeochemical Cycles, 27, 894-905. doi:10.1002/gbc.20080, 2013.

Lo Monaco, C., Metzl, N., Poisson, A., Brunet, C., and B. Schauer. Anthropogenic CO_2 in the Southern Ocean: Distribution and inventory at the Indian-Atlantic boundary (World Ocean Circulation Experiment line I6). Journal of Geophysical Research Oceans 110. doi:10.1029/2004JC002643, 2005.

Martin, J.H., Knauer, G.A., Karl, D.M., and W.W. Broenkow. VERTEX: Carbon cycling in the northeast Pacific. Deep-Sea Research I, 34, 267-285. doi.org/10.1016/0198-0149(87)90086-0, 1987.

Meyer, M.G., Gong, W., Kafrissen, S.M., Torano, O., Varela, D.E., Santoro, A.E., Cassar, N., Gifford, S., Niebergall, A.K., Sharpe, G., and A. Marchetti. Phytoplankton size-class contributions to new and regenerated production during the EXPORTS Northeast Pacific Ocean field deployment. Elementa Science of the Anthropocene 10. doi:10.1525/elementa.2021.00068, 2022b.

Meyer, M.G., Jones, R.M., and W.O. Smith Jr. Quantifying seasonal particulate organic carbon concentrations and export potential in the Southwestern Ross Sea using autonomous gliders. Journal of Geophysical Research, 127. doi:10.1029/2022JC018798, 2022a.

Misic, C., Bolinesi, F., Castellano, M., Olivari, E., Povero, P., Fusco, G., Saggiomo, M., and O. Mangoni. Factors driving the bioavailability of particulate organic matter in the Ross Sea (Antarctica) during summer. Hydrobiologia, 851, 2657-2679. doi.org/10.1007/s10750-024-05482-w, 2024.

Misic, C., Harriague, A.C., Mangoni, O., Aulicino, G., Castagno, P., and Y. Cotroneo. Effects of physical constraints on the lability of POM during summer in the Ross Sea. Journal of Marine Systems, 166, 132-143. doi.org/10.1016/j.jmarsys.2016.06.012, 2017.

Moreau, S., Mostajir, B., Belanger, S., Schloss, I.R., Vancoppenolle, M., Demers, S., and G.A. Ferreyra. Climate change enhances primary production in the western Antarctic Peninsula. Global Change Biology 21, 2191-2205. doi:10.1111/gcb.12878, 2015.

Morel, A. Optical properties of pure water and pure seawater. In Optical Aspects of Oceanography, edited by N.G. Jerlov & E. Steemann Nielsen, pp. 1-24, Academic, San Diego, CA, 1974.

Nelson, D.M., DeMaster, D.J., Dunabr, R.B., and W.O. Smith Jr. Cycling of organic carbon and biogenic silica in the Southern Ocean: Estimates of water-column and sedimentary fluxes on the Ross Sea continental shelf. Journal of Geophysical Research, 101, 18519-18532. doi:10.1029/96JC01573, 1996.

Niebergall, A.K., Traylor, S., Huang, Y., Feen, M., Meyer, M.G., McNair, H.M., Nicholson, D., Fassbender, A.J., Omand, M.M., Marchetti, A., Menden-Deuer, S., Tang, W., Gong, W., Tortell, P., Hamme, R., and N. Cassar. Evaluation of new and net community production estimates by multiple ship-based and autonomous observation in the Northeast Pacific Ocean. Elementa Science of the Anthropocene, 11. doi.org/10.1525/elementa.2021.00107, 2023.

Oxygen Optode 4831W/4831/4831F. https://www.aanderaa.com/media/pdfs/, last access: 16 December 2024.

Portela, E., Meyer, M.G., Smith, W.O., Jr., and K. Heywood. Unprecedented phytoplankton summer bloom in the Ross Sea. Geophysical Research Letters 52(3). doi.org/10.1029/2024GL111264, 2025.

Queste, B.Y., Heywood, K.J., Smith, W.O., Jr., Kaufman, D.E., Jickells, T.D., and M.S. Dinniman. Dissolved oxygen dynamics during a phytoplankton bloom in the Ross Sea polynya. Antarctic Science 27, 362-372. doi:10.1017/S0954102014000881, 2015.

Rousseau, V., Mathot, S., and C. Lancelot. Calculating carbon biomass of Phaeocystis sp. from microscopic observations. Marine Biology 107, 305-314, 1990.

Salaun, J., and M. Le Menn. In situ calibration of Wetlabs chlorophyll sensors: a methodology adapted to profile measurements. Sensors. doi:10.3390/s23052825, 2023.

Sanz Rodrigo, J., Buchlin, J.-M., van Beeck, J., Lenaerts, J.T.M., and M.R. van den Broeke. Evaluation of the Antarctic surface wind climate from ERA reanalyses and RACMO2/ANT simulations based on autonomatic weather stations. Climate Dynamics, 40 (1-2), 353-376. doi:10.1007/s00382-012-1396-y, 2012.

SBE 911 plus CTD. https://www.bodc.ac.uk/, last accessed: 16 December 2024.

Schine, C.M.S., van Dijken, G., and K.R. Arrigo. Spatial analysis of trends in primary production and relationship with large-scale climate variability in the Ross Sea, Antarctica (1997-2013). Journal of Geophysical Research: Oceans, 121, 368-386. doi.org/10.1002/2015JC011014, 2015.

Siegel, DA, Buesseler, KO, Behrenfeld, MJ, Benitez-Nelson, CR, Boss, E, Brzezinski, MA, Burd, A, Carlson, CA, D'Asaro, EA, Doney, SC, Perry, MJ, Stanley, RHR, and D.K. Steinberg. Prediction of the export and fate of global ocean net primary production: The EXPORTS science plan. Frontiers in Marine Science 3. doi:10.3389/fmar.2016.00022, 2016.

Smith, W.O., Jr., Ainley, D.G., Arrigo, K.R., and M.S. Dinniman. The oceanography and ecology of the Ross Sea. Annual Review of Marine Sciences, 6, 469-487. doi:10.1146/annurev-marine-010213-135114, 2014.

Smith, W.O., Jr., Asper, V.L., Tozzi, S., Liu, X., and S.E. Stammerjohn. Surface layer variability in the Ross Sea, Antarctica as assessed by in situ fluorescence measurements. Progress in Oceanography, 88, 28–45. doi.10.1016/j.pocean.2010.08.002, 2011.

Deleted: ,

Deleted: submitted.

Smith, W.O., Jr., and J.C. Comiso. Influence of sea ice primary production in the Southern Ocean: A satellite perspective. Journal of Geophysical Research, 113. doi:10.1029/2007JC004251, 2008.

Smith, W.O., Jr., and D.E. Kaufman. Climatological temporal and spatial distributions of nutrients and particulate matter in the Ross Sea. Progress in Oceanography, 168, 182-195. doi:10.1016/j.pocean.2018.10.003, 2018.

Smith, W.O., Jr., Marra, J., Hiscock, M.R., and R.T. Barber. The seasonal cycle of phytoplankton biomass and primary productivity in the Ross Sea, Antarctica. Deep-Sea Research II, 47, 3119-3140. doi.org/10.1016/S0967-0645(00)00061-8, 2000.

Smith, W.O., Jr., Tozzi, S., Long, M.C., Sedwick, P.N., Peloquin, J.A., Dunbar, R.B., Hutchins, D.A., Kolber, Z., and G.R. DiTullio. Spatial and temporal variations in variable fluorescence in the Ross Sea (Antarctica): Oceanographic correlates and bloom dynamics. Deep-Sea Research I, 79, 141-155. doi.org/10.1016/j.dsr.2013.05.002, 2013.

Steinberg, D.K., Carlson, C.A., Bates, N.R., Johnson, R.J., Michaels, A.F., and A.H. Knap. Overview of the US JGOFS Bermuda Atlantic Time-series Study (BATS): a decade-scale look at ocean biology and biogeochemistry. Deep Sea Research 48, 1405-1447. doi:10.1016/S0967-0645(00)00148-X, 2001.

Sweeney, C., Hansell, D.A., Carlson, C.A., Codispoti, L.A., Gordon, L.I., Marra, J., Millero, F.J., Smith, W.O., Jr., and T. Takahashi. Biogeochemical regimes, net community production and carbon export in the Ross Sea, Antarctica. Deep-Sea Research II, 47, 3369-3394. doi.org/10.1016/S0967-0645(00)00072-2, 2000.

Thomalla, S.J., Nicholson, S.-A., Ryan-Keogh, T.J., and M.E. Smith. Widespread changes in Southern Ocean phytoplankton blooms linked to climate drivers. Nature Climate Change 13, 975-984. doi:10.1038/s41558-023-01768-4, 2023.

Turner, J., Holmes, C., Harrison, T.C., Phillips, T., Jena, B., Reeves-Francois, T., Fogt, R., Thomas, E.R., & T.C.C. Bajish. Record low Antarctic sea ice cover in February 2022. Geophysical Research Letters 49. doi:10.1029/2022GL098904.

Wanninkhof, R. (2014), Relationship between wind speed and gas exchange over the ocean revisited. Limnology and Oceanography: Methods, 12, 351-362, 2022.

Yang, B., Emerson, S.R., and S.M. Bushinsky. Annual net community production in the subtropical Pacific Ocean from in situ oxygen measurements on profiling floats. Global Biogeochemical Cycles, 31, 728-744. doi:10.1002/2016GB005545, 2017.